

## **Microscale fracture of chromia scales**

Anand H.S. Iyer<sup>a</sup>, Gaurav Mohanty<sup>b,c</sup>, Krystyna Stiller<sup>a</sup>, Johann Michler<sup>c</sup>, Magnus Hörnqvist Colliander<sup>a</sup>

<sup>a</sup> Department of Physics, Chalmers University of Technology, Gothenburg, Sweden – 41296.

<sup>b</sup> Materials Science and Environmental Engineering, Tampere University, 33014, Tampere, Finland.

<sup>c</sup> Empa, Swiss Federal Laboratories for Materials Science and Technology, Laboratory for Mechanics of Materials and Nanostructures, Feuerwerkerstrasse 39, 3602 Thun, Switzerland.

### **Supplementary material**

#### **A. Residual stress evaluation by Raman spectroscopy**

The oxide scales were checked for the presence of residual stresses with Raman spectroscopy mapping in a WITec Alpha 300R Raman microscope. A green laser with wavelength of 532 nm was used in the Raman spectroscopy studies. Area scans were performed in order to obtain an idea of the spatial distribution of residual stresses. Due to the difference in coefficient of thermal expansion between metal and the oxide, stresses develop in the scale when it cools to room temperature after exposure. In addition to that, lateral growth stresses exist within the scale, resulting in a net residual stress in the oxide scale. In the case of chromia, the Raman spectrum consists of 2  $A_{1g}$  and 4  $E_g$  mode of vibrations [1], and the presence of stresses in the material causes a shift in the peak positions. For the  $A_{1g}$  peak near  $551\text{ cm}^{-1}$ , which is the most intense peak, the shift is linearly proportional to the stress. The formula for stress (in GPa) is described by:  $\sigma = -\Delta\nu \times 0.307$  [1], where  $\Delta\nu$  is the difference in wave number between the constrained oxide and the reference, and 0.307 is the shift stress

*Revised version submitted to Materialia. Different from the finally published version. May contain formatting, typographical and other errors.*

conversion coefficient. Figure S1 shows the Raman maps for the oxide scale. The residual stresses present in the oxide scale is compressive and as high as 1.8 GPa in some regions. The regions that appear dark in the figure are regions with larger faceted grains of oxide. The spatial resolution of Raman area mapping is roughly  $0.3\ \mu\text{m}$  and therefore the variation in stresses is clearer in the larger grains.

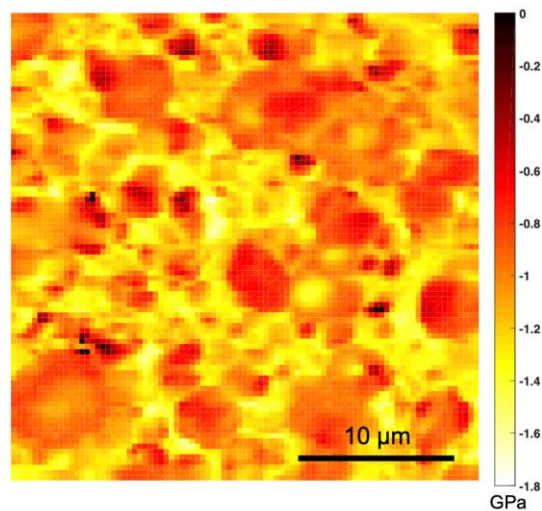


**Figure S1:** Raman map of the surface of oxide scale. Lighter regions have higher compressive residual stresses and darker regions have lower stresses.

## **B. Micro-cantilever dimensions**

**Table S1:** Dimensions of the FIB milled micro-cantilevers referred to as raw, where the top surface is untouched by ion-milling.

<b>Sl No:</b>	<b>Length</b> L ( $\mu\text{m}$ )	<b>Width</b> w ( $\mu\text{m}$ )	<b>Oxide depth</b> h ( $\mu\text{m}$ )	<b>Oxide span</b> $\chi$ ( $\mu\text{m}$ )
HT1	8.3 $\pm$ 0.03	3.23 $\pm$ 0.06	1.28 $\pm$ 0.19	2.94 $\pm$ 0.06
HT2	7.5 $\pm$ 0.02	2.94 $\pm$ 0.08	1.46 $\pm$ 0.54	2.88 $\pm$ 0.02
RT1	7.4 $\pm$ 0.06	5.4 $\pm$ 0.16	1.54 $\pm$ 0.26	2.96 $\pm$ 0.05
RT2	8.4 $\pm$ 0.05	5.28 $\pm$ 0.11	1.45 $\pm$ 0.35	2.9 $\pm$ 0.02
RT3	7.6 $\pm$ 0.04	4.29 $\pm$ 0.07	1.11 $\pm$ 0.08	2.98 $\pm$ 0.05

**Table S2:** Dimensions of micro-cantilevers referred to as flat, where the oxide surface is made smooth by ion-milling.

<b>Sl No:</b>	<b>Length</b> L ( $\mu\text{m}$ )	<b>Width</b> w ( $\mu\text{m}$ )	<b>Oxide depth</b> h ( $\mu\text{m}$ )	<b>Oxide span</b> $\chi$ ( $\mu\text{m}$ )
<b>F1</b>	8.63 $\pm$ 0.05	4.33 $\pm$ 0.02	1.2 $\pm$ 0.02	2.94 $\pm$ 0.03
<b>F2</b>	7.39 $\pm$ 0.04	4.41 $\pm$ 0.04	1.35 $\pm$ 0.04	3.1 $\pm$ 0.03
<b>F3</b>	8.82 $\pm$ 0.05	4.3 $\pm$ 0.03	1.12 $\pm$ 0.03	2.98 $\pm$ 0.05
<b>F4</b>	7.62 $\pm$ 0.04	4.2 $\pm$ 0.02	0.92 $\pm$ 0.02	2.9 $\pm$ 0.03

## **C. Stress-strain calculation using FEM**

Since the geometry of the milled micro-cantilevers were complex, the conversion of force-displacement data to stress-strain was done with the help of a finite element model with same

dimensions as the different micro-cantilevers. The surface roughness was not included and was considered as flat in the models. Figure S2 shows an example of the geometry used, consisting of half the cantilever and support with symmetry conditions enforced. A simple stationary study was performed on the model using dimensions of the different micro-cantilevers by application of an edge load,  $F/2$ .

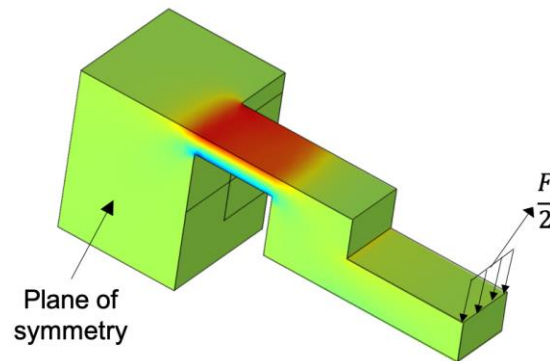


**Figure S2:** Geometry of micro-cantilever used in FEM.

The maximum stress ( $\sigma_{max}$ ) and strain ( $\varepsilon_{max}$ ) on the surface, and the displacement of the free end ( $\delta$ ) were evaluated and used in calculation of the geometric factors as follows:

$$k_{\sigma} = \frac{\sigma_{max}}{F}$$

$$k_{\varepsilon} = \frac{\varepsilon_{max}}{\delta}$$

The geometric factors were used to convert the experimental force-displacement data into stress and strain.

#### **D. Elastic modulus calculation**

Bending tests were conducted on flat micro-cantilevers by applying small displacements to avoid fracture. Each micro-cantilever was bent for at least two different displacements, and

each test consisted of three loading-unloading cycles in order to confirm repeatability. The force displacement data was converted to stress-strain by obtaining geometric constants from FEM (as in section C) and linear fitting in MATLAB was used to obtain the value of elastic modulus. Table S3 lists all the elastic modulus values obtained from the small displacement tests.

**Table S3:** Values of elastic modulus obtained from flat micro-cantilevers.

SI No:	Elastic modulus (GPa)
<b>F1</b>	257.3±19.8
<b>F2</b>	217.5±15.7
<b>F3</b>	301.3±15.1
<b>F4</b>	271.6±19.7

### **E. Anisotropy of elastic modulus**

In order to calculate the elastic anisotropy, the elastic stiffness in different crystallographic directions are required. In the case of Cr<sub>2</sub>O<sub>3</sub>, the following stiffness matrix was obtained from the values given in [2] considering rhombohedral symmetry:

$$C = \begin{bmatrix} 373 & 160 & 178 & -21 & 0 & 0 \\ 160 & 373 & 160 & 21 & 0 & 0 \\ 178 & 160 & 349 & 0 & 0 & 0 \\ -21 & 21 & 0 & 160 & 0 & 0 \\ 0 & 0 & 0 & 0 & 160 & -21 \\ 0 & 0 & 0 & 0 & -21 & 106.5 \end{bmatrix}$$

This matrix was used to calculate anisotropy with the aid of the web tool, ELATE [3]

(<http://progs.coudert.name/elate>).

*Revised version submitted to Materialia. Different from the finally published version. May contain formatting, typographical and other errors.*

The average elastic modulus (polycrystalline) was measured using Voigt averaging scheme,

$$E_{\text{avg}} = 318.2 \text{ GPa.}$$

Maximum value:  $E_{\text{max}} = 394.1 \text{ GPa.}$  (hkl= [0.67 0.37 -0.64])

Minimum value:  $E_{\text{min}} = 241 \text{ GPa.}$  (hkl = [0 0 1])

The anisotropy, which is the ratio of the maximum and minimum value is 1.63.

Figure S3 provides a visualisation of the anisotropy in elastic modulus ( $E$ ).

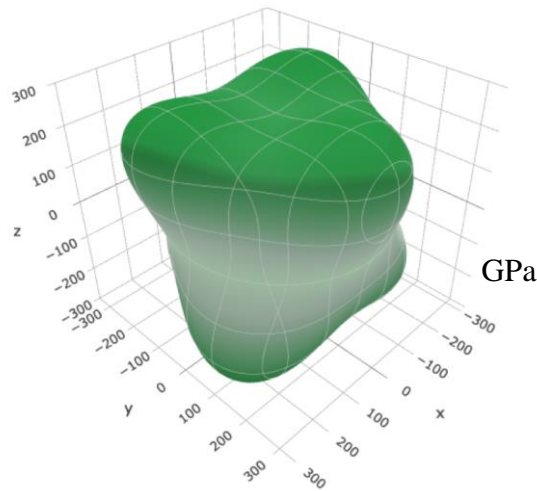


**Figure S3:** Visualisation of variation in elastic modulus for chromium oxide.

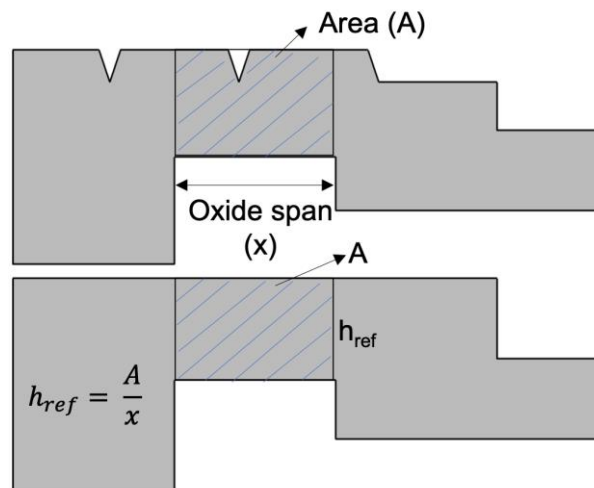
### **F. Effect of geometric irregularities evaluated using FEM**

Effect of the presence of features such as stress concentrations and porosity in the oxide scale on its stiffness was investigated with the help of elastic FE models. Some extreme cases were chosen in order to demonstrate how much variations in stiffness are caused by notches, bumps and porosities. The following procedure was used in each case evaluated:

- A geometry was generated based on the situation considered, such as presence of notch or porosity.
- A small force was applied the resulting displacement ( $\delta_n$ ) was measured.

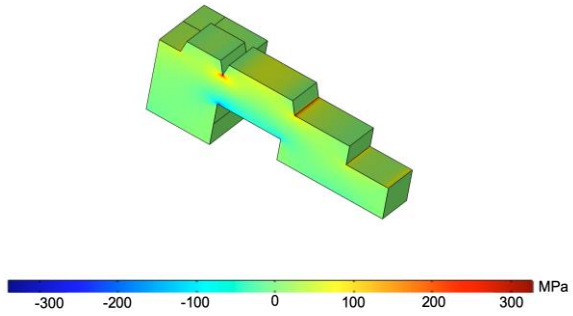
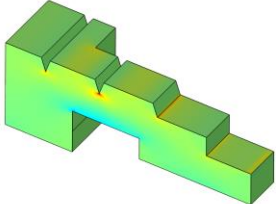
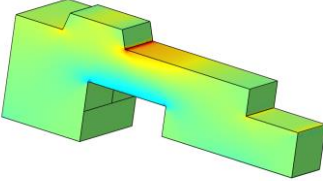
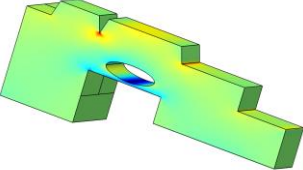
- A reference cantilever was generated without any notches/porosity, where the height of the oxide part of the cantilever was calculated by keeping the projected area at the oxide part as constant (shown in Figure S4).
- A similar procedure was followed on the reference cantilever as well, in order to obtain the displacement ( $\delta_{ref}$ ).
- The effect of the notch on stiffness ratio is calculated as  $\delta_{ref}/\delta_n$

Note that only the surface roughness was considered when calculating the equivalent reference area. The porosity was neglected in order to obtain stiffness ratios corresponding to those that would be measured experimentally, since pores were not accounted for when estimating the average thicknesses in Tables S1 and S2, and in the case of internal porosity it would not be known. The different cases considered are presented in Table S5, showing stiffness reductions in the order of 15–48 %. Although the extreme case is unlikely in practice the results show that significant geometrical effects on the deduced elastic moduli can be expected.

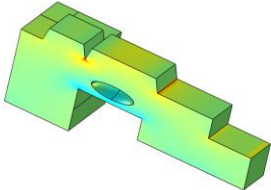


**Figure S4:** Illustration of how reference cantilever height is calculated.

**Table S5:** Different cases considered for FEM. The stress scale shown for the first case is common for all cases.

Case	Description	$\delta_{ref}/\delta_n$
	<p>Notch at support of cantilever.</p> <p>Notch height – 0.6 <math>\mu\text{m}</math> and width 0.4 <math>\mu\text{m}</math>.</p> <p>Height of oxide part – 2<math>\mu\text{m}</math></p> <p><math>h_{ref} = 1.98 \mu\text{m}</math></p>	0.65
	<p>Notch away from support.</p> <p>Notch height and width same as above.</p> <p><math>h_{ref} = 1.96 \mu\text{m}</math></p>	0.68
	<p>Bump at the support.</p> <p>Height – 0.6 <math>\mu\text{m}</math> total height - 2 <math>\mu\text{m}</math></p> <p><math>h_{ref} = 1.62 \mu\text{m}</math></p>	0.85
	<p>Notch at support and pore below.</p> <p>Notch is same size as above cases.</p> <p>Pore - ellipse with semi axes 1 and 0.3 <math>\mu\text{m}</math>.</p> <p><math>h_{ref} = 1.67 \mu\text{m}</math></p>	0.52



	Same as above but pore is internal. Pore- ellipsoid with semi axes 0.7, 1 and 0.3 $\mu\text{m}$ . $h_{\text{ref}} = 1.98 \mu\text{m}$	0.64
---	---	------

### **G. Analysis on redeposition layer**

Rough milling in FIB using high currents results in some redeposition on the surface of the oxide. In order to assess the presence of redeposition, A TEM lamella was prepared using FIB from a region near a milled micro-cantilever. High-resolution transmission electron microscopy (HRTEM) analysis was carried out in a FEI Titan 80-300 FEG TEM. High resolution imaging was performed in order to image the redeposition layer and assess its thickness as this layer would be amorphous, whereas the oxide grain would be crystalline.

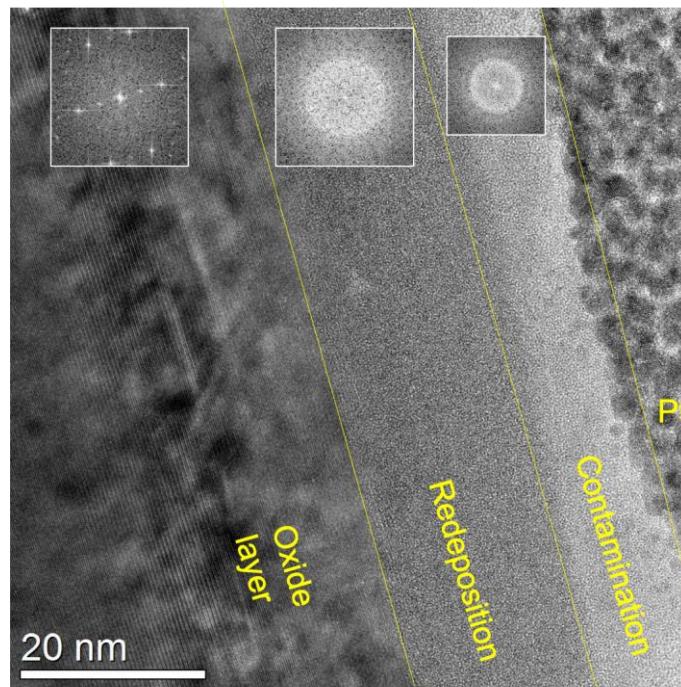


**Figure S6:** HRTEM image of chromium oxide layer with redeposition on top. The FFT is shown in inset for different layers.

Figure S6 shows the HRTEM image highlighting the different regions in the area of interest. From the fast fourier transforms (FFT) shown for different layers, it can be seen that the redeposition layer is amorphous and has a thickness of about 20 nm. Chemical analysis was done in the form of an energy dispersive X-Ray spectroscopy (EDX) line scan. Figure S7 shows the results of the EDX analysis, where it can be seen that the redeposition layer has a chemical composition similar to the oxide, which is expected since the redeposited material consists of the oxide and metal particles. The redeposition layer shows the presence of gallium in addition to chromium and oxygen, which also aids in highlighting the redeposited region.

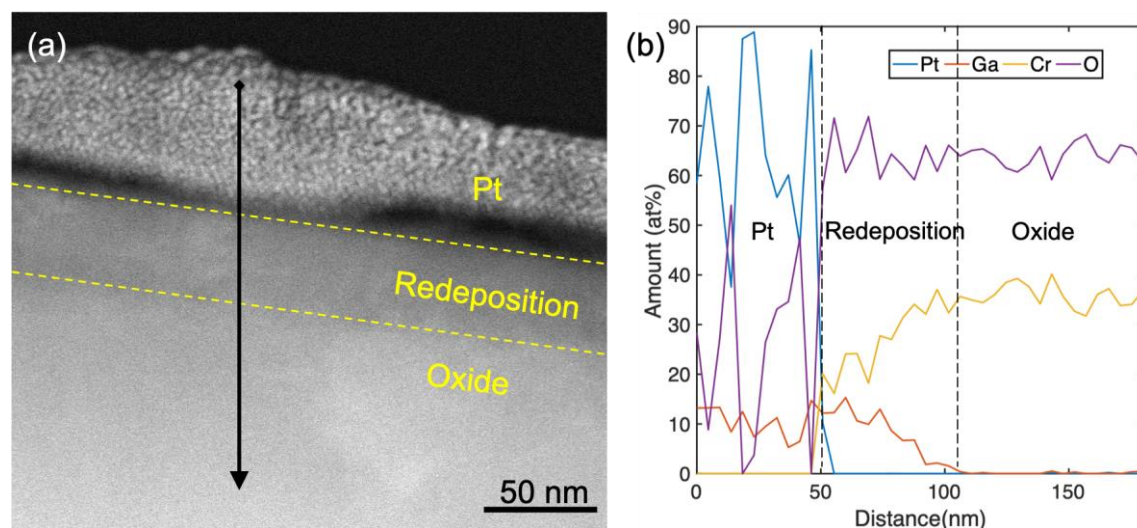


**Figure S7:** (a) High angle annular dark field (HAADF) scanning transmission electron microscopy (STEM) image of oxide layer with different regions highlighted; (b) results of EDX line scan from the black line shown in (a).

## References

- [1] J. Mougin, T. Le Bihan, G. Lucazeau, High-pressure study of  $\text{Cr}_2\text{O}_3$  obtained by high-temperature oxidation by X-ray diffraction and Raman spectroscopy, *J. Phys. Chem. Solids*. 62 (2001) 553–563. doi:10.1016/S0022-3697(00)00215-8.
- [2] Y. Wang, H. Fang, C.L. Zacherl, Z. Mei, S. Shang, L.Q. Chen, P.D. Jablonski, Z.K. Liu, First-principles lattice dynamics, thermodynamics, and elasticity of  $\text{Cr}_2\text{O}_3$ , *Surf. Sci.* 606 (2012) 1422–1425. doi:10.1016/j.susc.2012.05.006.
- [3] R. Gaillac, P. Pullumbi, F.X. Coudert, ELATE: An open-source online application for analysis and visualization of elastic tensors, *J. Phys. Condens. Matter*. 28 (2016). doi:10.1088/0953-8984/28/27/275201.